Biochemistry

 Volume 39, Number 43 October 31, 2000

Articles

Heme Structure of Hemoglobin M Iwate [α87(F8)His→Tyr]: A UV and Visible Resonance Raman Study†

M. Nagai,*,‡ M. Aki,§ R. Li,‡ Y. Jin,‡ H. Sakai,|| S. Nagatomo,⊥ and T. Kitagawa*,§,⊥

School of Health Sciences, Kanazawa University Faculty of Medicine, Kodatsuno, Kanazawa 920-0942, Japan, School of Mathematical and Physical Science, Graduate University for Advanced Studies, Myodaiji, Okazaki 444-8585, Japan, Sakai Womens Clinic, Itsukaichi, Iwate 028-4307, Japan, and Institute for Molecular Science, Okazaki National Research Institutes, Myodaiji, Okazaki 444-8585, Japan

Received May 5, 2000; Revised Manuscript Received August 11, 2000

ABSTRACT: Heme structures of a natural mutant hemoglobin (Hb), Hb M Iwate [α87(F8)His→Tyr], and protonation of its F8-Tyr were examined with the 244-nm excited UV resonance Raman (UVRR) and the 406.7- and 441.6-nm excited visible resonance Raman (RR) spectroscopy. It was clarified from the UVRR bands at 1605 and 1166 cm^{-1} characteristic of tyrosinate that the tyrosine (F8) of the abnormal subunit in Hb M Iwate adopts a deprotonated form. UV Raman bands of other Tyr residues indicated that the protein takes the T-quaternary structure even in the met form. Although both hemes of α and β subunits in metHb A take a six-coordinate (6c) high-spin structure, the 406.7-nm excited RR spectrum of metHb M Iwate indicated that the abnormal α subunit adopts a 5c high-spin structure. The present results and our previous observation of the $\nu_{Fe-O(tyrosine)}$ Raman band [Nagai et al. (1989) *Biochemistry 28*, 2418−2422] have proved that F8-tyrosinate is covalently bound to Fe(III) heme in the α subunit of Hb M Iwate. As a result, peripheral groups of porphyrin ring, especially the vinyl and the propionate side chains, were so strongly influenced that the RR spectrum in the low-frequency region excited at 406.7 nm is distinctly changed from the normal pattern. When Hb M Iwate was fully reduced, the characteristic UVRR bands of tyrosinate disappeared and the Raman bands of tyrosine at 1620 (Y8a), 1207 (Y7a), and 1177 cm^{-1} (Y9a) increased in intensity. Coordination of distal His(E7) to the Fe(II) heme in the reduced α subunit of Hb M Iwate was proved by the observation of the ν_{Fe-His} RR band in the 441.6-nm excited RR spectrum at the same frequency as that of its isolated α chain. The effects of the distal-His coordination on the heme appeared as a distortion of the peripheral groups of heme. A possible mechanism for the formation of a Fe(III)−tyrosinate bond in Hb M Iwate is discussed.

The existence of familial cyanosis having an autosomal dominant inheritance pattern has been recognized in Iwate

† This work was supported in part by the Grant-in-Aid for scientific research to M.N. (10670115) and to T.K. (10480187) from the Ministry of Education, Science, Culture and Sports of Japan.

* Address correspondence to either author. Phone, +81-564-55-7340; fax, +81-564-55-4639; e-mail, teizo@ims.ac.jp (T.K.). Phone, +81-76-265-2581; fax, +81-76-234-4360; e-mail, nagai@kenroku.kanazawa-u.ac.jp (M.N.).

‡ Kanazawa University Faculty of Medicine.

10.1021/bi001029i CCC: $19.00
Published on Web 09/29/2000

Prefecture, Japan, since 1800. The affected individuals have a "lavender-blue" appearance, while their blood is brownish. It was revealed that they have an abnormal hemoglobin (Hb)[1] named "Hb M Iwate" in addition to normal Hb (Hb A). The hemolysate has an absorption spectrum that is similar to but not identical with that of methemoglobin A (metHb A). The structure of Hb M Iwate was first analyzed by Shibata et al. (*1*), and the subsequent X-ray study (*2*) indicated that Hb M Iwate remained in the T-quaternary structure even in the fully oxidized form. Disability to switch to the R-structure upon oxygen binding to the normal β subunit explains the low oxygen affinity and the absence of Bohr effect in this Hb variant. It was not clear in the X-ray analysis with 5.5-Å resolution whether the heme group interacts with the tyrosine at F8 (proximal) or with histidine at E7 (distal). The studies with ^{1}H NMR (*3*, *4*) and resonance Raman spectroscopy (*5*, *6*) suggested that the heme iron of the abnormal α subunit is coordinated only to tyrosine (F8) in the physiological conditions, but when it is reduced chemically in the presence of CO (*7*), the His-coordinated CO heme is generated. However, it is unclear whether the Fe(III) heme binds to F8-tyrosine or tyrosinate; furthermore, evidence for the Fe(II)−E7 histidine bonding remains to be presented.

In the present study, using a new type of UV resonance Raman (UVRR) spectrometer (*8*) with a solar-blind multichannel detector and a quasi-CW UV laser source (244 nm), we demonstrate that F8-tyrosine in the abnormal subunit of Hb M Iwate is ionized (tyrosinate) in the normal condition. The effects of Fe(III)−tyrosinate bonding on the heme structure were examined by 406.7-nm excited resonance Raman (RR) spectroscopy. Changes of F8-tyrosine and the heme upon reduction were examined by 244-nm excited UVRR and 441.6-nm excited RR spectroscopy, respectively.

EXPERIMENTAL PROCEDURES

Hemoglobins. Hb A was purified from fresh human blood by preparative isoelectric focusing electrophoresis using 5% ampholine (pH 6−9) (*9*). Hb M Iwate was separated from Hb A by an Amberlite CG-50 column chromatography (*10*). Isolated chains of Hb A and Hb M Iwate were prepared in the following way. Hemoglobin was split into chains by adding *p*-chloromercuribenzoate (PMB) (*11*, *12*). The α-PMB and β-PMB chains were separated by an isoelectric focusing electrophoresis on a Sephadex G-75 superfine gel bed containing 5% ampholine, pH 3.5−9.5. The PMB of α and β chains were removed by adding dithiothreitol (3 mg/mL) in 0.1 M Tris buffer, pH 8.2, and then passed through a Sephadex G-25 column. The isolated chains were oxidized by ferricyanide to met form, and after removal of ferricyanide, it was equilibrated with 1 M glycine, pH 7.0, based on the method of Banerjee et al. (*13*). For UVRR measurements, ca. 0.2 mL of 200 μM (in terms of heme) Hb solution in 0.1 M phosphate buffer (pH 7.0) containing 0.01 M sodium perchlorate was put into a small rubber-top spinning cell (diameter 5 mm). The deoxy form of Hb M Iwate was obtained by adding sodium dithionite (2 mg/mL) to the hemoglobin solution after replacement of the inside air with N_2 gas and standing overnight at room temperature (*10*). The Raman band of ClO_4^- ions at 932 cm^{-1} was used as an internal intensity standard for the calculation of difference spectra.

Measurements of UV Resonance Raman Spectra. UV Resonance Raman (UVRR) spectra were excited by the second harmonic of a mode-locked Ar^+ ion laser system (Spectra Physics, model 2045 and model 451) operated at ∼82 MHz with an average pulse-width of 100 ps and power of ∼1 W. The second harmonic was generated with a BBO (β-BaB_2O_4) crystal with an average power of ∼1 mW and focused to a diameter of 50 μm at the sample by a lens (f = 100 mm). The average power of the 244-nm line at the sample was reduced to ∼220 μW (∼6.2×10^{-7} J/cm^2·pulse) by a neutral density filter. The scattered light at right angle was collected by a UV microscope lens (Zeiss, Ultrafluar 10×, NA = 0.20, WD = 7.4 mm) and focused onto the entrance slit of the spectrograph (SPEX 1269, f = 1260 mm, F = 9) by an achromatic lens (f = 200 mm). A liquid filter, which is butyl acetate/methanol mixed solution [methanol: butyl acetate = 4:1 (v/v)] contained in a 10 mm thick rectangular cuvette, was placed behind the objective lens to reject the Rayleigh scattering.

Raman spectra was dispersed with a blazed-holographic grating with 3600 grooves/mm blazed at 250 nm and focused onto the CsTe photocathode of an intensified charge coupled device (ICCD, Princeton Instruments, model ICCD-1024MG-E/1), which was cooled to −29 °C. Since the CsTe photocathode has sensitivity only between 200 and 300 nm, it rejects visible fluorescence from the sample, if any. The CCD has 1024 × 256 pixels, but the central 700 × 256 pixels were used because of a limited size of a microchannel plate intensifier. The wavenumber coverage is ca. 560 cm^{-1}, and thus 1 pixel corresponds to ∼0.8 cm^{-1}, that is the wavenumber resolution of this measurement. Raman shifts were calibrated with a cyclohexane and cyclohexane/trichloroethylene mixed solution [cyclohexane:trichloroethylene = 4:1 (v/v)] as a standard. The spectral intensity was corrected with a D_2 standard lamp (Hamamatsu, model C1518 and model H4141SV). Details of the UVRR measurement system is reported separately (*8*).

Since UV laser light is focused into the sample solution to efficiently collect Raman scattering, the protein might be denatured if an identical molecule is illuminated repeatedly even under spinning. To protect the sample from denaturation, a spinning cell (diameter = 5 mm, 600 rpm), which made it possible to stir the sample solution during spinning of the cell, was newly designed (*8*) and used in this study. A small magnetic stirring bar was put into a spinning cell and kept to a stand still at the bottom near the side wall of the cell by an outside fixed magnet. The effective agitation of the spinning solution in fact took place by the inside magnet bar and protected the Hb sample from denaturation by UV laser illumination.

The temperature of the sample solution was kept at 15 °C by flushing with cooled N_2 gas against the spinning cell. One UVRR spectrum was a sum of ∼120 exposures, each exposure accumulating the data for 60−30 s. Integrity of the sample after the exposure to the UV laser light was

§ Graduate University for Advanced Studies.
|| Sakai Womens Clinic.
⊥ Okazaki National Research Institutes.

[1] Abbreviations: Hb, hemoglobin; RR, resonance Raman; UVRR, UV resonance Raman; PMB, *p*-chloromercuribenzoate; 5c and 6c, five- and six-coordinated hemes.

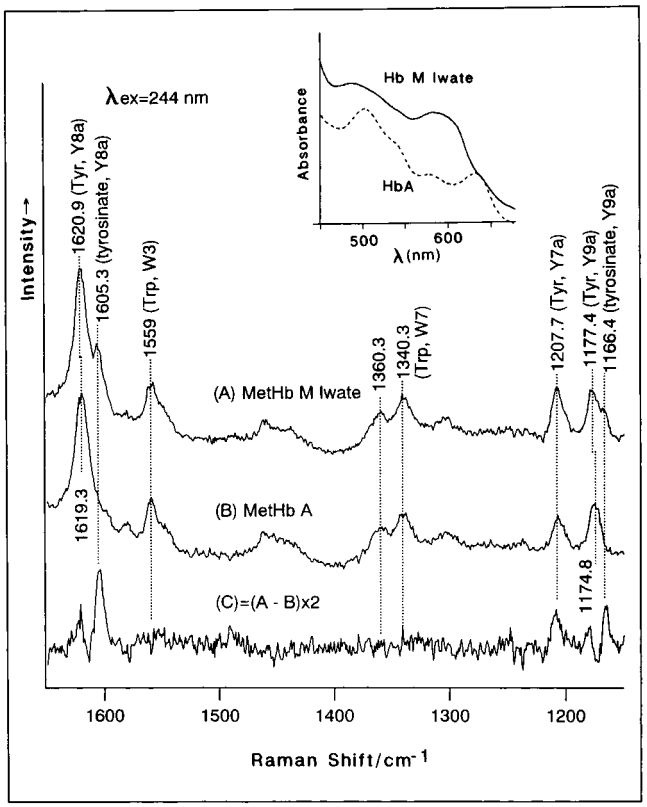

FIGURE 1: 244-nm excited UV resonance Raman spectra of metHb M Iwate (A), metHb A (B), and their difference spectrum (C). The concentration of Hbs was 200 μM (in heme) in 0.1 M phosphate buffer, pH 7.0, containing 0.01 M sodium perchlorate. The Raman difference spectrum, which was obtained by subtracting the Raman spectrum of metHb A from that of metHb M Iwate so that the 932 cm^{-1} band of perchlorate becomes zero, is 2-fold expanded in the ordinate scale. Inset shows the absorption spectra of metHb M Iwate (—) and metHb A (- - -) used for the measurements of UVRR spectra.

carefully confirmed by the visible absorption spectra measured before and after the UVRR measurements. If some spectral changes were recognized, the Raman spectrum was discarded. Visible absorption spectra were measured with a Hitachi 220S spectrophotometer.

Measurements of Visible Resonance Raman Spectra. Visible RR scattering was excited with the 441.6-nm line of a He/Cd laser (Kinmon Electric, model CD4805R) or the 406.7-nm line of a Kr^+ laser (Spectra-Physics model 164) and recorded on a JEOL-400D Raman spectrometer equipped with a cooled photomultiplier (RCA-31034a). Raman spectra for examining the H/D substitution effects on deoxyHb were excited at 441.6 nm, dispersed with a 100-cm single polychromator (Ritsu Oyo Kogaku, model MC-100DG), and detected with a cooled CCD detector (Princeton Instruments, UV/CCD-1340/400). All measurements were carried out at room temperature with an ordinary spinning cell (1800 rpm). Laser power at the sample point was 4.0 mW. Raman shifts were calibrated with indene (500−1600 cm^{-1}) (*14*) and CCl_4 (200−500 cm^{-1}).

RESULTS

UV Resonance Raman Spectrum of metHb M Iwate. Figure 1 shows the 244-nm excited UVRR spectra of metHb M Iwate (A), metHb A (B), and their difference (C = Hb M Iwate − Hb A) in the frequency region from 1650 to 1150 cm^{-1}. The absorption spectra of Hbs used for the UVRR measurements are depicted in the inset of Figure 1. In the RR spectrum of Hb A (B), Raman bands of Tyr were observed at 1619 (Y8a, ring C−C stretch), 1208 (Y7a, $C_\beta C_\alpha$ stretch), and 1175 cm^{-1} (Y9a, ring C−H bend); those of Trp were seen at 1559 (W3) and 1360−1340 cm^{-1} (W7, tryptophan doublet), respectively. These assignments are based on the results of Harada and co-workers (*15*, *16*). In the spectrum of Hb M Iwate (A), two extra Raman bands are observed at 1605 and 1166 cm^{-1} in addition to the usual RR bands of Tyr. The peak at 1208 cm^{-1} is intensified. This is more clearly seen in the difference spectrum (C), which reveals differential type peaks for ordinary Tyr bands at 1620 and 1175 cm^{-1} in addition to the new bands at 1605 and 1166 cm^{-1}.

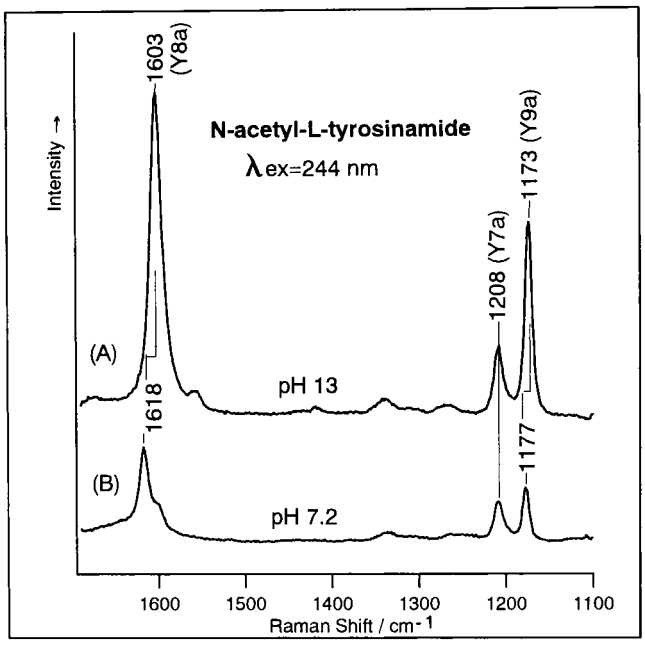

FIGURE 2: 244-nm excited UV resonance Raman spectra of *N*-acetyl-L-tyrosinamide at pH 13 and pH 7.2. The concentration of *N*-acetyl-L-tyrosinamide was 10 mM in 0.1 M NaOH (pH 13) and in 0.1 M phosphate buffer (pH 7.2).

To identify these new RR bands, the RR spectrum of *N*-acetyl-L-tyrosinamide at pH 13 is compared with that at pH 7.2 in Figure 2. RR bands for un-ionized Tyr at pH 7.2 (B) are observed at 1618 (Y8a), 1208 (Y7a), and 1177 cm^{-1} (Y9a), but those for ionized Tyr (tyrosinate) at pH 13 (A) are seen at 1603 (Y8a), 1208 (Y7a), and 1173 cm^{-1} (Y9a). The Y8a and Y9a bands are shifted to lower frequencies and greatly intensified upon deprotonation, while the Y7a band is not shifted but slightly intensified. Accordingly, the extra bands found in the spectrum of Hb M Iwate are considered to arise from a tyrosinate. The Y9a peak is seen at 1173 cm^{-1} for the tyrosinate solution contrary to 1166 cm^{-1} for Hb M Iwate. Since the Y9a frequency is known to be sensitive to a displacement of the OH hydrogen atom from the plane of benzene ring (*17*), the downshift of Y9a for Hb M Iwate may be influenced by the O^-−Fe(III) bonding.

Since appreciable high-frequency shifts of Y8a and Y9a RR bands are recognized for the R → T-quaternary structure transition of Hb A in the 244-nm excited RR spectrum, the

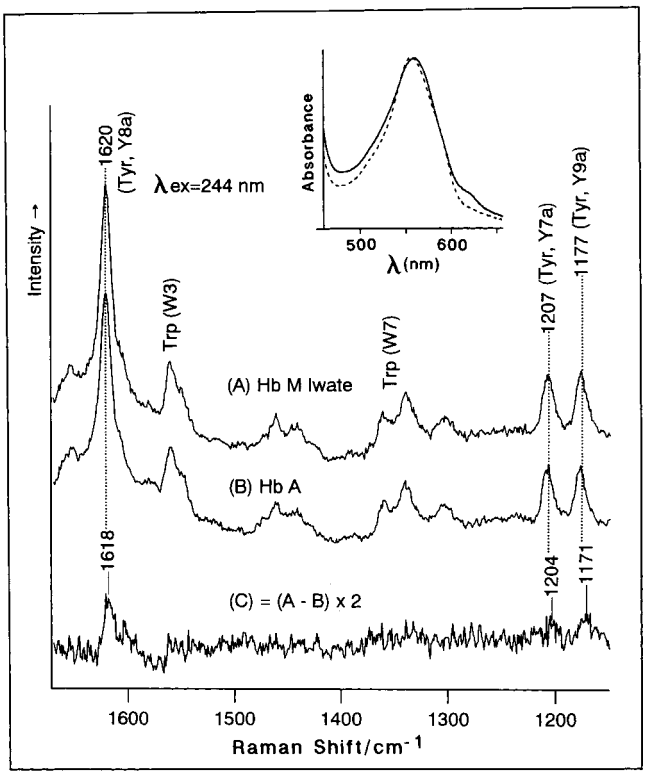

FIGURE 3: 244-nm excited UV resonance Raman spectra of the fully reduced Hb M Iwate (A), deoxyHb A (B), and their difference spectrum (C). The concentration of the reduced Hb M Iwate and deoxyHb A was 200 μM (in heme) in 0.1 M phosphate buffer, pH 7.0, containing 2 mg of sodium dithionite/mL and 0.01 M sodium perchlorate. The Raman spectrum was obtained under anaerobic conditions. Inset shows the absorption spectra of the fully reduced Hb M Iwate (—) and deoxyHb A (- - -) used for the measurements of UVRR spectra.

upshifts of the Y8a and Y9a bands from 1619 and 1175 cm^{-1} in Hb A to 1621 and 1177 cm^{-1} in Hb M Iwate, as revealed by difference spectrum (Figure 1C), presumably indicate that Hb M Iwate maintains the T conformation even in the fully met form. However, the intensity enhancement of Trp RR bands on the R → T transition found in the 229- and 235-nm excited UVRR spectra (*9*, *18*) was not prominent in the 244-nm excited UVRR spectrum. The changes of Trp RR bands in the 235-nm excited UVRR spectrum due to the hydrogen bond formation of β37Trp with α94Asp in deoxyHb A were caused possibly by a red-shift of B_b absorption band from 220 to 235 nm (*19*, *20*), but the Raman excitation at 244 nm may not be on resonance with the B_b band.

UVRR Spectrum of the Fully Reduced Hb M Iwate. Although the reduction of abnormal met-α subunit of Hb M Iwate is difficult, the fully reduced Hb M Iwate could be obtained by standing with 2 mg of dithionite/mL in anaerobic conditions overnight at room temperature. The absorption spectrum of reduced Hb M Iwate was similar to that of deoxyHb A as compared in the inset of Figure 3. The 244-nm excited UVRR spectrum of reduced Hb M Iwate (A) is compared with that of deoxyHb A (B) in Figure 3, where their difference is illustrated by spectrum C. The characteristic RR bands of tyrosinate at 1605 and 1166 cm^{-1} observed for metHb M Iwate (Figure 1A) disappeared and the peaks of tyrosine at 1620, 1207, and 1177 cm^{-1} increased in intensity as compared with those of deoxyHb A. The difference spectrum (Figure 3C) between the reduced Hb M Iwate and deoxyHb A revealed the spectrum of F8-Tyr, which is close to that of un-ionized tyrosine in Figure 2. This result indicates that the tyrosinate−Fe(III) bond in metHb M Iwate was broken upon reduction, and then the tyrosinate was changed to a tyrosine.

RR Spectra of Hb M Iwate in the Fully Met Form and the α*-met/*β*-*deoxy *Form.* Figure 4 depicts the 406.7-nm excited RR spectra of the fully met form (metHb M Iwate) (A), α-met and β-deoxy form of Hb M Iwate (B), and metHb A (C) in the 1680−1250 cm^{-1} (left) and 530−180 cm^{-1} regions (right). Because of the resonance condition, the 406.7-nm excitation mainly enhances the Raman bands of ferric heme, and accordingly, the contribution from deoxyheme is small. Although the RR spectrum of the fully met form of Hb M Iwate (Figure 4A) includes the contributions from both abnormal α-met and normal β-met hemes, the spectrum of α-met and β-deoxy form of Hb M Iwate (Figure 4B) reflects only the abnormal α-met subunit in Hb M Iwate. Therefore, the weighted addition of spectra B and C would qualitatively reproduce spectrum A.

On the basis of the RR spectra in the high-frequency region, where the marker bands for the oxidation (ν_4), spin (ν_2, ν_3), and coordination states (ν_2, ν_3) of heme iron appear (*21*, *22*), the hemes of metHb A and metHb M Iwate are considered to adopt the high-spin state. The ν_3 peak of metHb A at 1480 cm^{-1} reflects the six-coordinated (6c) high-spin structure in which a water molecule is weakly coordinated to the Fe(III) ion as the sixth ligand (*23*−*27*). On the other hand, the ν_3 and ν_2 bands of the fully met form of Hb M Iwate are shifted to higher frequencies to 1488 and 1570 cm^{-1}, respectively. It is deduced from the spectrum of α-met and β-deoxy form of Hb M Iwate that the shifted bands mainly arise from the abnormal α subunit. The upshifts of these bands are associated with a smaller core size of the 5c high-spin heme (*23*−*27*).

Raman bands in the lower frequency region have been assigned as indicated in Figure 4 (*28*, *29*). The pyrrole tilting mode (ν_9) around 260 cm^{-1} (*29*−*31*), the out-of-plane methine wagging mode (γ_7) around 300 cm^{-1}, and the pyrrole stretching and substituent bending mode (ν_8) at 343 cm^{-1} are little shifted between metHb M Iwate and metHb A. On the contrary, the Raman bands involving the $C_\beta-C_c-C_d$ bending character of the propionate methylene groups [$\delta(C_\beta C_c C_d)$] at 370−380 cm^{-1} and the $C_\beta-C_a-C_b$ bending character of the vinyl groups [$\delta(C_\beta C_a C_b)$] at 410−426 cm^{-1} are distinctly different between metHb M Iwate and metHb A. Thus, the characteristic RR bands of met-α subunit of Hb M Iwate appear at 426 [$\delta(C_\beta C_a C_b)_{2,4}$] and 370 cm^{-1} [$\delta(C_\beta C_c C_d)_{6,7}$], while those of metHb A are present at 411 and 381 cm^{-1}, respectively. The apparent RR spectral changes of Hb M Iwate in the lower frequency region imply a distortion of heme peripheral groups of abnormal α-met subunit, especially in the vinyl and propionic groups (*29*).

Effects of pH on the RR Spectra. RR spectra of metHb A and metHb M Iwate at pH 5 and pH 10 were examined. The RR spectra of metHb A are altered appreciably with pH. Upon increase of pH, the ν_4 band shifts from 1372 to 1376 cm^{-1}, and the ν_3 band shifts from 1482 to 1478 cm^{-1}. The acidic and alkaline forms of metHb A are characterized by the sixth ligand of the heme iron, which is H_2O at pH 5 (high-spin) and OH^- at pH 10 (low/high-spin mixture) (*32*).

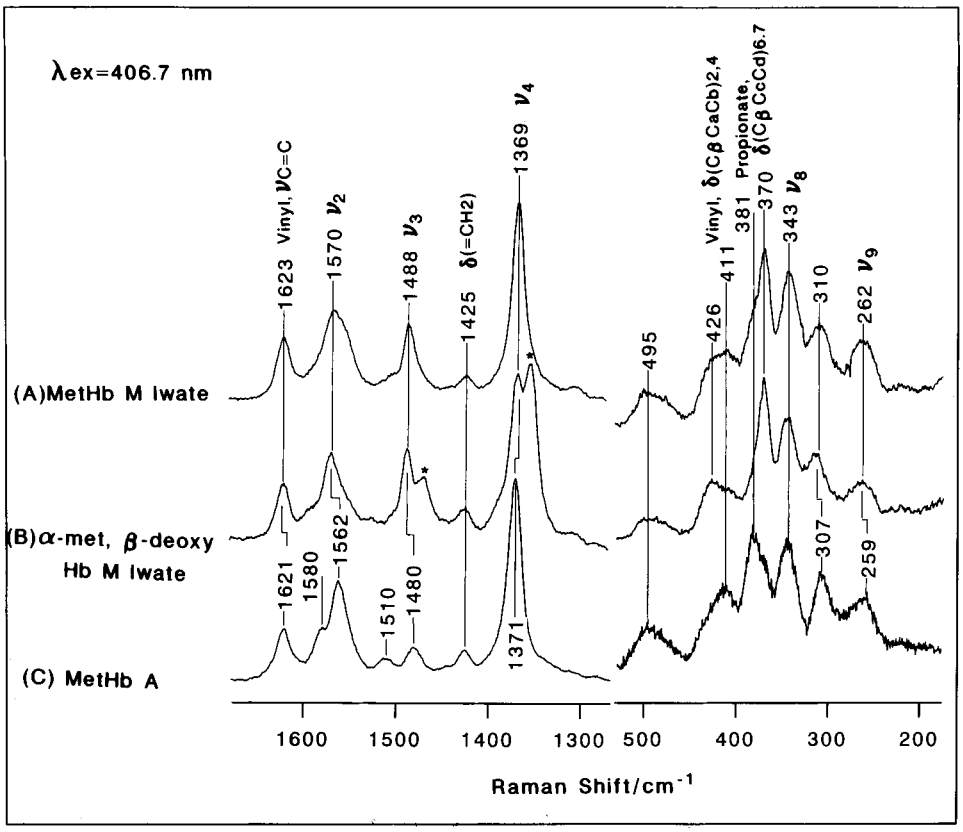

FIGURE 4: 406.7-nm excited resonance Raman spectra of metHb M Iwate (A), α-*met*,*β*-deoxy Hb M Iwate (B), and metHb A (C). The concentration of Hbs was 100 μM (in heme) in 0.1 M phosphate buffer, pH 7.0. The α-*met*,*β*-deoxy Hb M Iwate was prepared by photodissociation of CO from α-*met*,*β*-CO Hb M Iwate. An asterisk denotes Raman bands from the deoxy*β* subunit.

The intensity ratio of two Raman bands, I(1582 cm^{-1})/I(1564 cm^{-1}), has been noted to reflect the relative concentration of the low- and high-spin states of the heme (*33*). Indeed, the pH dependence of this ratio for metHb A is consistent with the expected increase of the low-spin heme at higher pH. In the lower frequency region, several modes including $\delta(C_\beta C_c C_d)$, γ_7, and ν_9 reduced in intensity at pH 10. The vinyl bending mode, $\delta(C_\beta C_a C_b)$, was greatly upshifted from 407 cm^{-1} at pH 5 to 430 cm^{-1} at pH 10. In contrast, the RR spectra of metHb M Iwate changed slightly upon an increase of pH (data not shown). Although small intensity changes are present around ~1560 and ~410 cm^{-1} due to the changes of normal met-*β* subunit in Hb M Iwate, the abnormal met-α subunit is considered to maintain the 5c high-spin structure of heme even at pH 10.

Isolated Chains and Reconstitution. Figure 5 compares the 406.7-nm excited RR spectrum of the met-α chain (α^M) isolated from Hb M Iwate with that of the normal met-α chain (α^A) isolated from Hb A. The normal met-α chain gave a RR spectrum (Figure 5B) different from that of metHb A (Figure 4C). The RR spectrum of α^A in the high-frequency region is close to that of alkaline metHb A, for which the RR band of the 6c low-spin heme is intensified at 1578 (ν_2) as compared with that for the 6c high-spin species (1564 cm^{-1}). In the low-frequency region, the propionate sensitive modes and ν_9 are different from those of metHb A: 378 and 267 cm^{-1} for α^A (Figure 5B) and 381 and 259 cm^{-1} for metHb A (Figure 4C). The RR spectrum of the isolated normal met-*β* chain was similar to that of the normal met-α chain (data not shown). In contrast, the RR spectrum of the isolated met-α chain of Hb M Iwate (Figure 5A) is similar to that of Hb M Iwate tetramer (Figure 4B). Comparison of the RR spectra between α^M and α^A indicates significant upshifts of the ν_3 and ν_2 bands to 1489 and 1573 cm^{-1}, respectively, which reflect the smaller core size associated with the 5c high-spin heme.

Figure 6 shows the RR spectra of the tetramer reconstituted with the isolated α and *β* chains. When the isolated normal α and *β* chains were mixed, the RR spectrum (Figure 6B) changed greatly in the ν_2 and ν_3 region and became similar to that of metHb A. The digital sum of the spectra of the isolated normal α and *β* chains are displayed by Figure 6A for comparison. On the other hand, when the met-α chain of Hb M Iwate and normal met-*β* chain were mixed, the spectrum represented by Figure 6D was obtained. Small but significant frequency shifts were also observed for ν_2, ν_4, $\delta(C_\beta C_a C_b)$, and γ_7, and the resultant spectrum became similar to native metHb M Iwate and also to the digital sum of the spectra of isolated abnormal α and normal *β* chains as shown by Figure 6C.

RR Spectrum of the Fully Reduced Hb M Iwate. Figure 7 compares the 441.6-nm excited RR spectrum of the fully reduced Hb M Iwate with that of deoxyHb A. The spectral patterns of deoxyHb A and fully reduced Hb M Iwate are alike, although peak positions and relative intensities are slightly different. A prominent peak was observed at 216 cm^{-1} for reduced Hb M Iwate. This band is reminiscent of the ν_{Fe-His} mode. As this intensity is more than half of that in deoxyHb A, it suggests that the heme iron of the abnormal α subunit in the reduced Hb M Iwate also binds to His. If distal His binds to the heme iron, there would be significant structural changes in the heme pocket of the abnormal

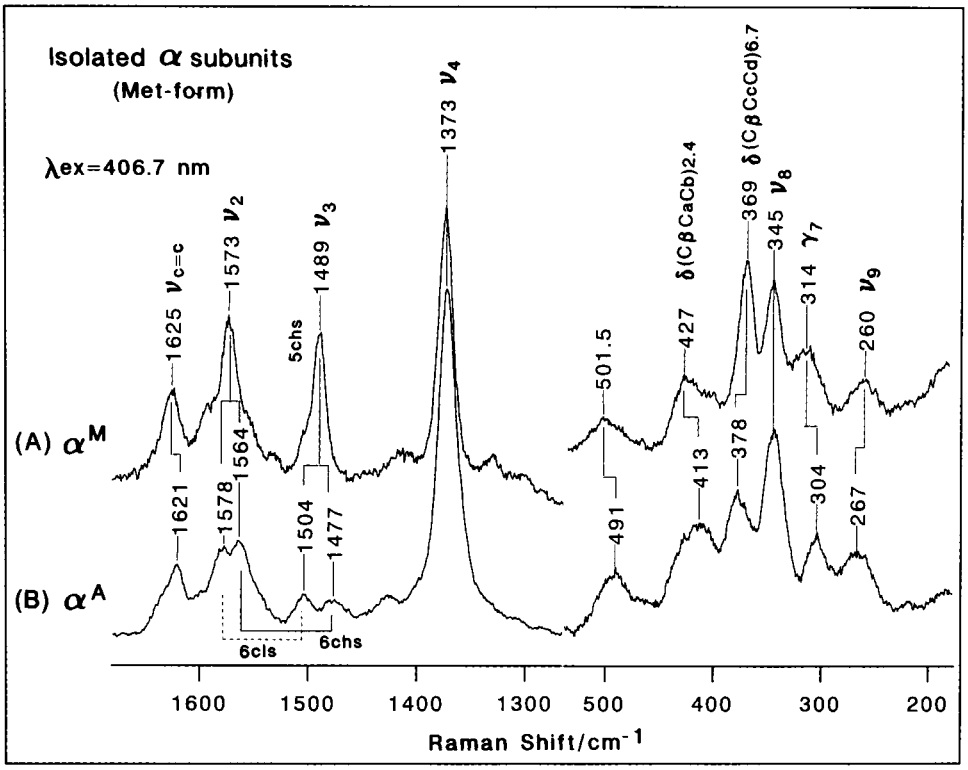

FIGURE 5: 406.7-nm excited resonance Raman spectra of the isolated α subunit from Hb M Iwate (A) and from Hb A (B) in met form. The concentration of subunits was 100 μM (in heme) in 0.05 M phosphate buffer, pH 7.0, containing 1 M glycine.

subunit, causing appreciable spectral differences between Hb A and Hb M Iwate in the low-frequency region. Then, the appearance of an intense band at 253 cm^{-1} for reduced Hb M Iwate would be understandable. Accordingly, we examined the reduced forms of the isolated abnormal α and normal β chains of Hb M Iwate.

Isolated Chains. To get a direct evidence for the coordination of distal histidine (E7-His) to Fe(II) in the abnormal subunit of reduced Hb M Iwate, the RR spectrum of the isolated α chain from Hb M Iwate (α^M) in the reduced form was measured and compared with that of the α chain (α^A) isolated from Hb A in Figure 8. The RR spectra of α^M (A) and α^A (B) are quite alike. In the spectrum of α^M, a clear peak was observed at 216 cm^{-1}, and it is assigned to the ν_{Fe-His} mode. Usually the ν_{Fe-His} band of the isolated chain appears at 222 cm^{-1} similar to that of deoxyMb, and the frequency reflects the R conformation (*34*). The RR spectrum of the isolated β chain was similar to that of α chain (data not shown). However, the ν_{Fe-His} frequency for the reduced Iwate α chain was as low as that of deoxyHb A, suggesting the presence of some strain in the Fe(II)−His bond of Iwate α chain in the same way as that in the T conformation. Other spectral differences between Iwate α and normal α chains are seen for the γ_7 (297 vs 300 cm^{-1}) and vinyl-related bands (404/1617 vs 404−429/1619 cm^{-1}). The Raman band at 253 cm^{-1} observed for the reduced Hb M Iwate was not identified in the spectrum of the isolated Iwate α chain. To examine a possibility that the 253-cm^{-1} band appears upon incorporation into the tetramer, the RR spectra of reconstituted tetramers were explored.

Figure 9 compares the RR spectra of the recombined tetramer, which were obtained through mixing of the isolated α and β chains, with a digital sum of the spectra of isolated α and β chains. When normal α and β chains were mixed (Figure 9B), some RR spectral changes are recognized for ν_4, ν_2, and ν_3 bands in the high-frequency region in comparison with that of digital sum (Figure 9A). In addition, the ν_{Fe-His} frequency is downshifted from 222 to 216 cm^{-1}. This is due to the quaternary structure changes from the R to T conformation. On the other hand, in the case of the recombined tetramer obtained from Iwate α and normal β chains, spectral changes in the high-frequency region were small (Figure 9C,D). However, the spectral changes in the low-frequency region are larger. The frequency of the ν_{Fe-His} mode is also downshifted from 220 (calculated mean) to 216 cm^{-1} (mix). This apparent shift is due to the β chain, which adopts the R conformation in the isolated form but T conformation in the tetramer, while the α chain retains the T conformation in both. The prominent intensity increase of the peak at 254 cm^{-1} seems to be characteristic of the recombined Hb M Iwate. A similar RR band is seen at 257 cm^{-1} in the spectrum of the recombined Hb A but is not distinct.

Smulevich et al. (*35*) suggested that the RR band at 269 cm^{-1} of reduced cytochrome *c* peroxidase appeared from an internal mode of histidine ligand, because the peak at 269 cm^{-1} was downshifted by 3 cm^{-1} in D_2O. To examine the H/D effect on 253-cm^{-1} band in the reduced Hb M Iwate, the RR spectra of the reduced Hb M Iwate and deoxyHb A were carefully measured in H_2O and D_2O. As shown in Figure 10, the frequencies of the ν_{Fe-His} mode of Hb A and Hb M Iwate were downshifted by 2−3 cm^{-1} in D_2O solution more than those in H_2O, but the 256-cm^{-1} band for Hb A and 253-cm^{-1} band for Hb M Iwate were the same between the H_2O and D_2O buffer solutions, indicating that the 253-cm^{-1} band of Hb M Iwate was not related to the histidine mode.

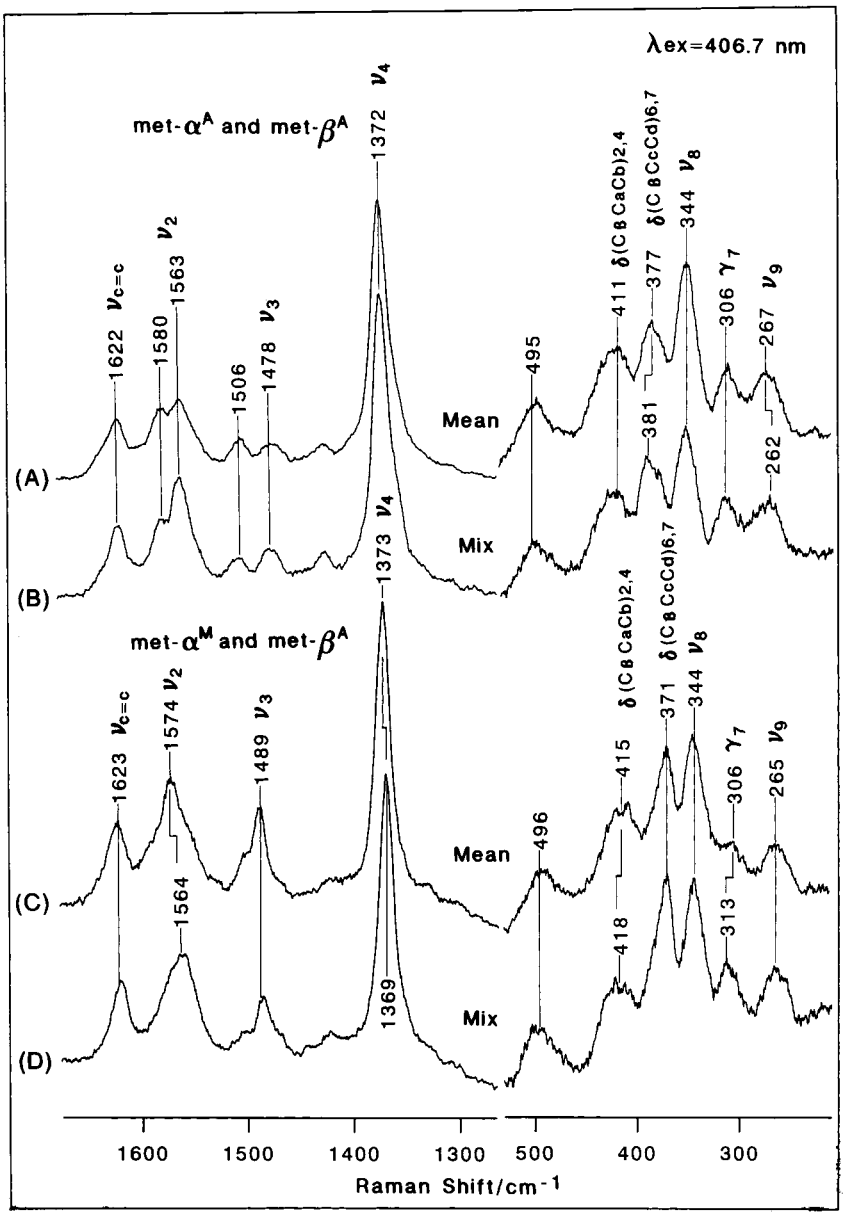

FIGURE 6: 406.7-nm excited resonance Raman spectra of recombined tetramers of Hb A and Hb M Iwate in the met form. (A) Digital sum of the spectra of α^A and β^A subunits observed before their mixing (mean). (B) Spectrum of recombined α^A and β^A subunits (mix). (C) Digital sum of the spectra of α^M and β^A subunits observed before their mixing (mean). (D) Spectrum of recombined α^M and β^A subunits (mix). The concentration of subunits used was 100 μM (in heme) in 0.05 M phosphate buffer, pH 7.0, containing 1 M glycine.

To determine whether the 253-cm^{-1} band of the reduced Hb M Iwate arises from α or β subunits, the spectrum of α-met,β-deoxy Hb M Iwate was examined with the same excitation line, and the result is depicted by Figure 10E. This spectrum resembles spectrum A. The 253-cm^{-1} band is not observed for this tetramer, meaning that the 253-cm^{-1} band of reduced Hb M Iwate arises from the abnormal α subunit. It is likely that this mode arises from ν_9 (pyrrole tilting) (*27*, *30*). In addition, these data show that the 294-cm^{-1} band (γ_7, out-of-plane methine wagging) of the reduced Hb M Iwate arises from the α subunit, because the band was not clear in the spectrum of α-met,β-deoxy Hb M Iwate.

DISCUSSION

From the 5.5-Å resolution X-ray studies of Hb M Iwate, it is suggested that both the distal (E7) His and proximal (F8) Tyr coordinate to the heme iron of Iwate α subunit (*2*). EPR spectrum of Hb M Iwate resembles to that of metHb A, although the signal height of metHb M Iwate is about 10-fold larger than that of metHb A (*37*). This has been attributed to the narrowing of the band possibly due to reduced interactions between electron spins of the heme iron and nuclear spins of the ligand (*37*). The ^{1}H NMR studies (*3*, *4*) suggest that the heme iron of the abnormal α subunit in Hb M Iwate is coordinated by F8-Tyr, but when it is reduced and bound to CO, the heme iron is then bound to the E7-His. Resonance Raman study (*5*) has demonstrated that the abnormal α subunit in Hb M Iwate adopts the 5c form with Tyr as an axial ligand. More recent Raman studies (*6*, *7*) have revealed that all four Hbs M (Hb M Iwate, Hb M Boston, Hb M Hyde Park, and Hb M Saskatoon) exhibit the fingerprint bands characteristic of the Fe−tyrosine proteins (*38*), and the characteristic Raman bands of Tyr-coordination disappear upon reduction. However, it is unclear

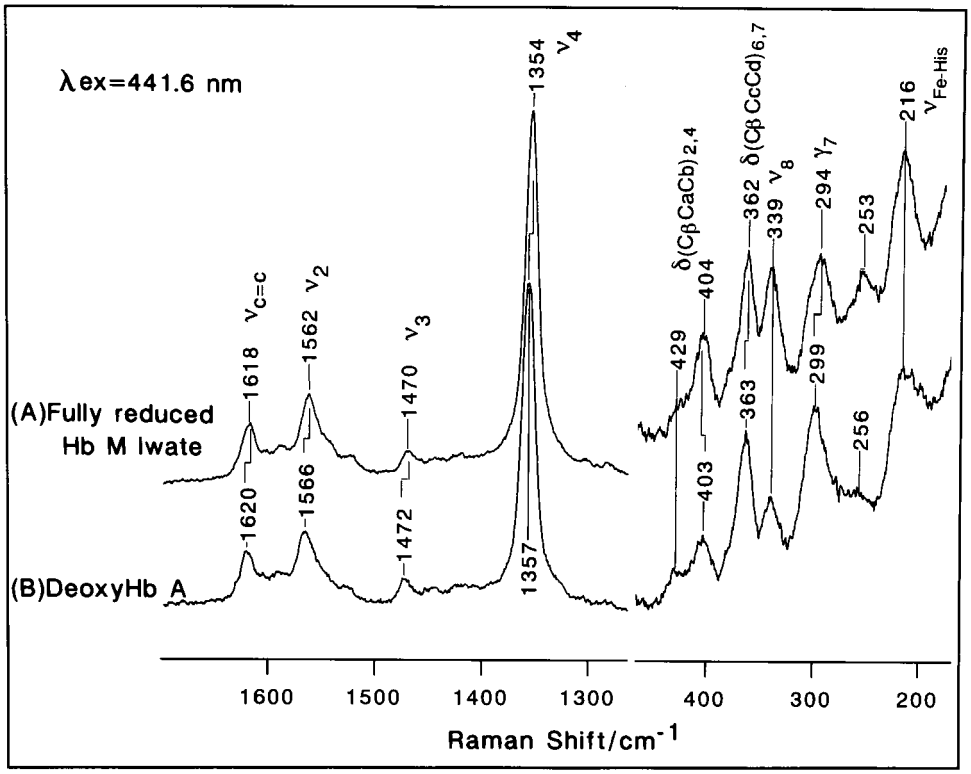

FIGURE 7: 441.6-nm excited resonance Raman spectra of the fully reduced Hb M Iwate (A) and deoxyHb A (B). The concentration of Hbs was 100 μM (in heme) in 0.1 M phosphate buffer, pH 7.0, containing 2 mg of sodium dithionite/mL. Raman spectrum was measured under anaerobic conditions.

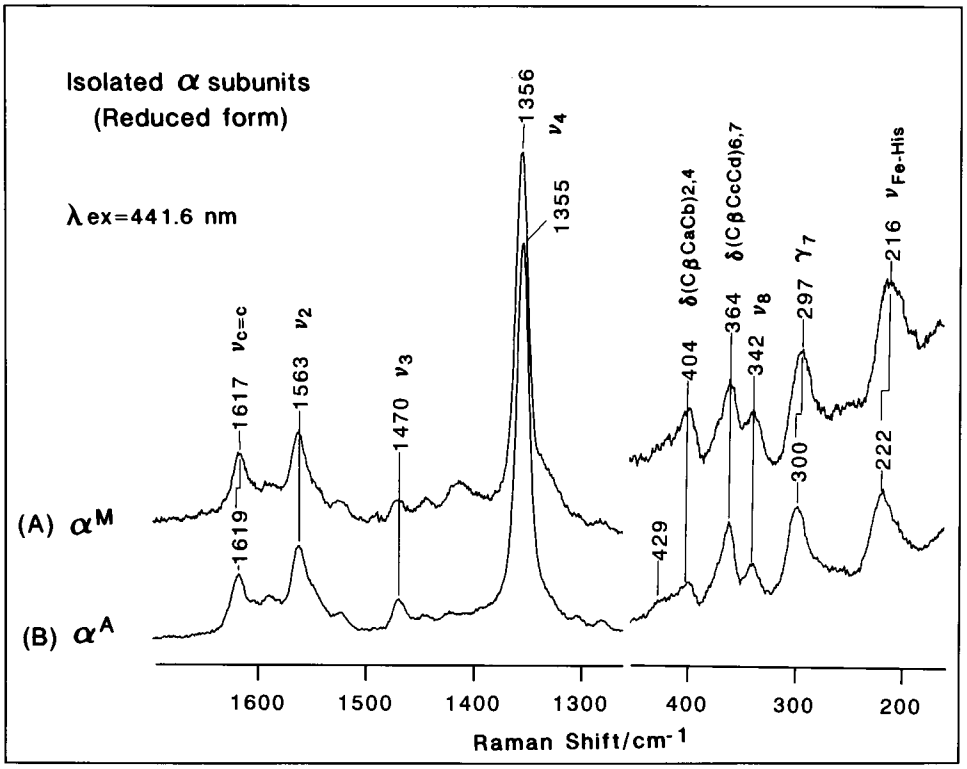

FIGURE 8: 441.6-nm excited resonance Raman spectra of the isolated α subunit from Hb M Iwate (A) and from Hb A (B) in the deoxy form. The concentration of subunits was 100 μM (in heme) in 0.1 M phosphate buffer, pH 7.0. Other conditions were the same as in Figure 7.

about protonation of the F8-Tyr in the abnormal α subunit in metHb M Iwate and its possible change upon reduction. The E7-His coordination in the reduced Hb M Iwate has not yet been established.

UV Resonance Raman. The direct evidence for the presence of a tyrosinate in Hb M Iwate has been provided for the first time in this study by the 244-nm excited UVRR spectroscopy. The Raman bands of tyrosinate were intensity

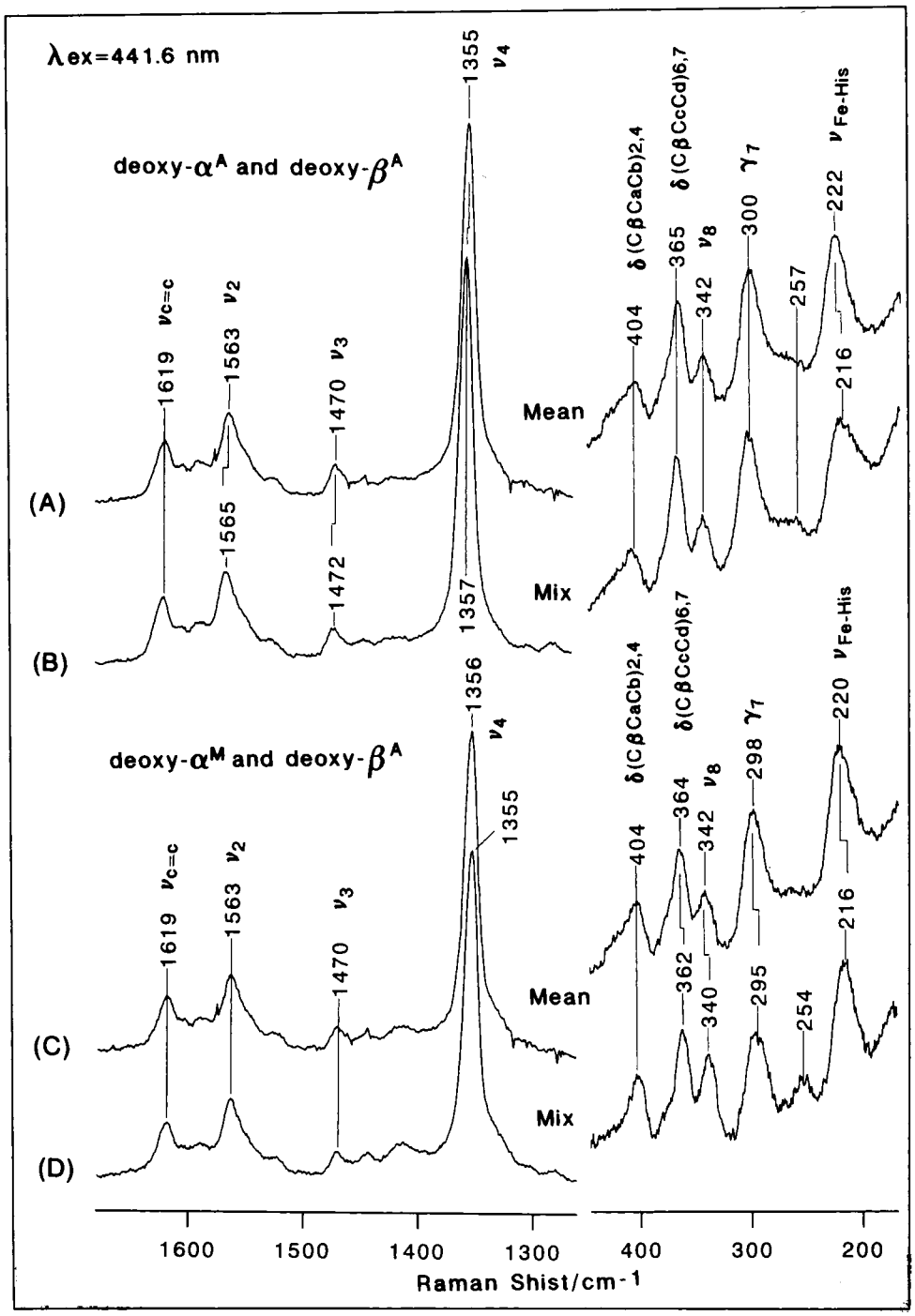

FIGURE 9: 441.6-nm excited resonance Raman spectra of recombined tetramers of Hb A and Hb M Iwate in the deoxy form. (A) Digital sum of the spectra of α^A and β^A subunits observed before their mixing (mean). (B) Spectrum of recombined α^A and β^A subunits (mix). (C) Digital sum of the spectra of α^M and β^A subunits observed before their mixing (mean). (D) Spectrum of recombined α^M and β^A subunits (mix). The concentration of subunits used was 100 μM (in heme) in 0.1 M phosphate buffer, pH 7.0.

enhanced at 1605 (Y8a, ring-C−C stretching), 1208 (Y7a, ring-Cext stretching), and 1166 cm^{-1} (Y9a, C−H bend) in resonance with the L_a transition (*39*). This was confirmed by the observation of the corresponding tyrosinate RR bands for alkaline *N*-acetyl-L-tyrosinamide at 1603 (Y8a), 1208 (Y7a), and 1173 cm^{-1} (Y9a) (Figure 2). The Y9a frequency of tyrosinate in the spectrum of Hb M Iwate is lower than that of the model compound by 7 cm^{-1}. Although Y9a is mainly associated with the in-plane CH bend, it would probably involve appreciable contribution from the C−O stretch, and the downshift of Y9a would be caused by differences between Fe−O⁻C and H···O⁻C bonding at oxygen, which results in a change of the C−O bond strength.

Comparison of the frequencies of ordinary Tyr of metHb A with those of metHb M Iwate (Figure 1) indicated small upshifts of Y8a and Y9a frequencies for metHb M Iwate. Usually the quaternary structure of metHb A is similar to that of liganded Hb (R structure), for which the Y8a and Y9a frequencies are 2−3 cm^{-1} downshifted as compared with those for deoxyHb (T structure) (*40*). This means that Hb M Iwate maintains the T-quaternary structure even in the met form.

When Hb M Iwate was reduced by dithionite, RR bands of the tyrosinate disappeared and the intensity of RR bands

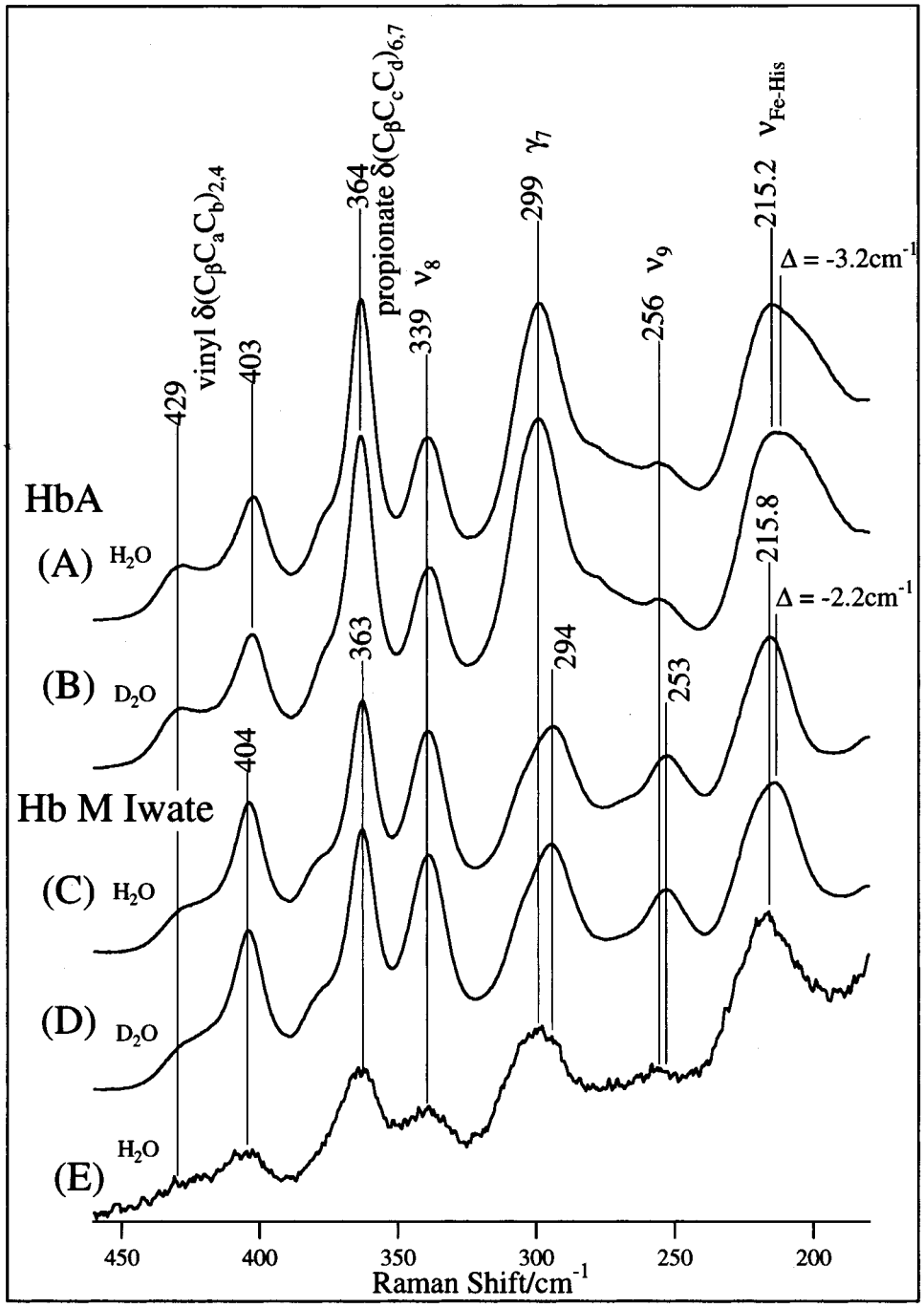

FIGURE 10: H/D effects on the 441.6-nm excited resonance Raman spectra of deoxyHb A (A and B), fully reduced Hb M Iwate (C and D), and half-reduced Hb M Iwate (E). The concentration of Hbs was 100 μM (in heme) in either 0.1 M phosphate buffer, pH 7.0, or pD 7.0. (A) DeoxyHb A in H_2O buffer. (B) DeoxyHb A in D_2O buffer. (C) Fully reduced Hb M Iwate in H_2O buffer. (D) Fully reduced Hb M Iwate in D_2O buffer. (E) Half-reduced Hb M Iwate [α^M-*met*,β^A-deoxy] in H_2O buffer. Spectra A−D were measured with a 100-cm single polychromator and a cooled CCD detector, whereas spectrum E was recorded on a JEOL-400D Raman spectrometer with a cooled photomultiplier.

for un-ionized Tyr increased. The RR spectrum for un-ionized F8-Tyr could be extracted from the raw spectra by difference calculations as depicted by Figure 3C. All the RR bands of F8-Tyr in the reduced Hb M Iwate are lower by 2−5 cm^{-1} than those of other Tyr residues. The frequency of RR bands of Tyr is influenced by hydrophobicity of its surroundings and H-bond formation; especially the formation of an H-bond in hydrophobic environments makes the frequency downshifted and the intensity increased (*41*). This suggests that F8-Tyr in reduced Hb M Iwate forms a strong H-bond with nearby residues in a hydrophobic heme pocket without forming a chemical bond with Fe(II).

Effects of the Tyrosinate−Fe(III) Bond Formation on the Heme Structure. In the high-frequency region of the 406.7-nm excited RR spectrum, Hb M Iwate shows intense RR bands of a 5c high-spin heme structure (Figure 4). Similar spectral features were also noted in the spectra of human mutant Mb (H93Y) (*42*) and whale heart mutant Mb (H93Y) (*43*). Here, we stress that the formation of tyrosinate−Fe(III) bond brings about distinct effects on the RR spectrum in the low-frequency region, especially in the propionate and vinyl substituents of porphyrin ring. The propionate mode,

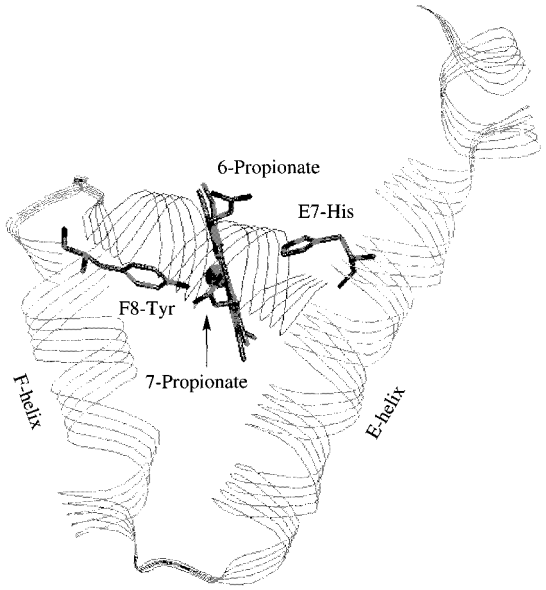

FIGURE 11: Main-chain arrangements and orientation of amino acid side chains of the proximal (F8) tyrosine and the distal (E7) histidine in mutant Mb (HF8Y). X-ray crystallographic coordinates were taken from the Protein Data Bank (*44*).

$\delta(C_\beta C_c C_d)$, which appears at 381 cm^{-1} for Hb A, is significantly downshifted to 370 cm^{-1} for Hb M Iwate. The vinyl mode, $\delta(C_\beta C_a C_b)$, which appears at 411 cm^{-1} for Hb A, is upshifted by 15 cm^{-1} (to 426 cm^{-1}) for Hb M Iwate. Presumably, these changes indicate geometrical distortion of the substituents in Hb M Iwate due to slight movement of the heme group toward F helix by the strong coordination of F8-Tyr.

High-resolution X-ray crystallographic structure is not available for the H(F8)Y mutant Hb but was recently reported for the H(F8)Y mutant of horse heart Mb by Hildebrandt et al. (*44*). In the H(F8)Y mutant Mb, the overall folding of polypeptide chain is found to be similar to that of the wild-type protein except for the region around the mutation site and its associated helix (F helix) as illustrated in Figure 11. The hydroxyl oxygen of Tyr93 occupies the position of the normally resident $N_{\epsilon 2}$ atom of His93 and is bound to the heme iron as an axial ligand. The plane of the Tyr93 phenyl group is rotated by 71° relative to the plane of the imidazole ring present in the wild-type protein, and the H-bonding network of the propionate is greatly affected (*44*). These results of mutant Mb are probably applicable to the α subunit of Hb M Iwate.

Distal Histidine Ligation to Fe(II). Previously we showed that the 441.6-nm excited RR spectrum of fully reduced Hb M Iwate yielded the clear ν_{Fe-His} mode, suggesting that both α and β subunits in Hb M Iwate have the Fe(II)−His bond (*7*). However, it was questioned whether the distal (E7) His is coordinated to the heme iron in the α subunit, because the RR band of ν_{Fe-His} can arise from the β subunit. To answer this question, we examined the RR spectrum of the isolated α subunit of Hb M Iwate. Generally isolation of abnormal subunits from Hbs M is hard. Among five Hbs M, an isolated subunit could be obtained without denaturation only from Hb M Iwate, while abnormal subunits of all other Hbs M were denatured during the chain separation procedure (unpublished work). Because of this fact, reconstitution experiments with the isolated chain are indispensable to confirm occurrence of no irreversible changes.

The ν_{Fe-His} Raman band for the reduced H(F8)Y mutant Mb was extremely weak (*42*) or lacking (*43*), indicating that the E7-His coordination to the heme iron is difficult in the H(F8)Y mutant Mbs. However, as shown in Figure 8A, the reduced α subunit of Hb M Iwate exhibited a prominent RR band of the ν_{Fe-His} mode at 216 cm^{-1}, indicating the coordination of E7-His to the heme iron. There were some effects of the E7-His ligation on the heme structure. The vinyl- and propionate-related Raman bands and γ_7 were changed (Figure 7). In addition, the prominent 253-cm^{-1} band was observed in the spectrum of the reduced Hb M Iwate. However, this band was absent in the spectrum of isolated α subunit but appeared upon recombination of the abnormal α with normal β subunits (Figure 9).

There are different assignments for the RR band at ∼260 cm^{-1}. Nissum et al. (*45*) assigned the ∼260-cm^{-1} bands of cytochrome *c* peroxidase and ascorbate peroxidase to an internal mode of proximal His, because its frequency was shifted in the D_2O solution. On the other hand, Choi and Spiro (*30*) proposed that the 255-cm^{-1} band in the spectra of a model compound $[(ImH)_2Fe(III)(OEP)]Cl$ arose from the pyrrole tilting mode on the basis of the frequency shift observed for ^{56}Fe substitution. Teraoka and Kitagawa (*36*) observed a band at 257 cm^{-1} for 2MeIm-d_5−Fe(II)PP and 2MeIm-d_5−Fe(II)OEP and noted that these bands were insensitive to d_5 substitution of axial 2MeIm, while the ν_{Fe-Im} frequency was shifted by the d_5 substitution. We confirmed that the 253-cm^{-1} band in the fully reduced Hb M Iwate was not affected by the H/D exchange of the buffer solution (Figure 10). Therefore, its assignment to ν_9 (*36*) or the pyrrole tilting mode (*30*) seems more plausible. As the 253-cm^{-1} RR band was not obvious in the spectrum of α-met,β-deoxy Hb M Iwate (Figure 10E) as well as of isolated α-deoxy Iwate (Figure 8), the appearance of this RR band may reflect a particular strained structure of heme group characteristic of the α subunit of Hb M Iwate in the tetrameric form. In the spectra of deoxyHb A, the band at 257 cm^{-1} slightly increases in intensity upon recombination of the α with β subunits (Figure 9), although the tendency is less obvious than that for Hb M Iwate. The ν_9 mode of Mb is sensitive to the H-bonding of the propionate at position 7 (*46*). Accordingly, the appearance of ν_9 might be related with distortion of heme associated with a particular geometry of the propionate side chain at position 7.

Mechanism of Fe(III)−Tyrosinate Bond Formation in Hb M. The fully reduced Hb M Iwate does not form an Fe−Tyr bond. However, after removal of dithionite by gel filtration or dialysis, the oxidation of the heme iron of Hb M Iwate proceeded rapidly in air, and it was followed by the formation of Fe(III)−tyrosinate bond (unpublished observation). Reduction of the reformed Fe(III)−tyrosinate is very hard as mentioned above. What is a mechanism for the Fe(III)−Tyr^- bond formation from the Fe(II) heme and un-ionized tyrosine? The oxidation of Fe(II), subsequent ionization of Tyr residue, and rapid Fe(III)−tyrosinate formation is reminiscent of biomineralizaton in ferritin. The reaction for incorporation of ferrous iron to apoferritin requires oxygen, and the incorporated iron is present in the ferric state in ferritin showing a purple color. The purple color of ferritin is identified to be due to the Fe(III)−tyrosinate bonding (*47*). The incorporation reaction of Fe(II) to apoferritin is very

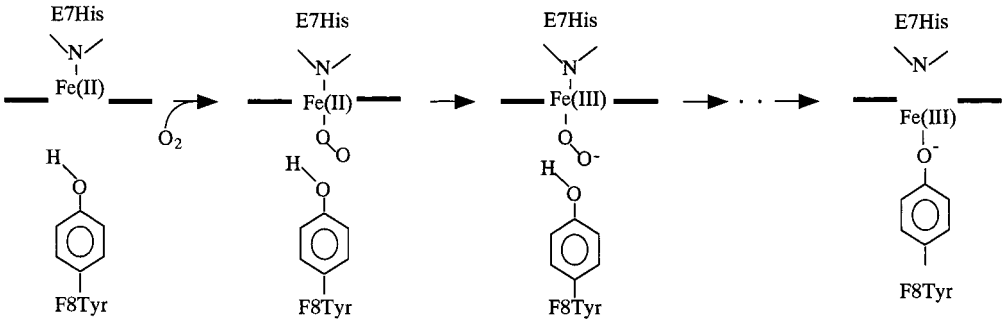

FIGURE 12: Possible mechanism of the formation of the Fe(III)−tyrosinate bond in Hb M Iwate.

rapid but does not occur in anaerobic conditions. In this biomineralization, consumption of O_2 and uptake of Fe(II) proceed in a stoichiometric way (*48*).

In the case of Hb M Iwate, the substituted Tyr for His(F8) in nascent globins may be present in an un-ionized form and keeps the heme iron in the ferrous form, which is probably bound to the distal (E7) His. When oxygen binds to the abnormal α subunit, rapid oxidation of heme iron and the subsequent formation of the Fe(III)−tyrosinate bond must proceed as illustrated in Figure 12. In the previous paper, we showed the presence of the reduced abnormal subunits in patient's blood with Hb M Saskatoon and Hb M Boston by EPR (*49*) and IR (*50*). This is another evidence supporting the scheme of Figure 12. Recent IR study has revealed the presence of O−O stretching band around 1100 cm^{-1} for intermediates in autoxidation of Hb and Mb, suggesting that normal oxy-heme with the Fe(III)−O_2^- structure serves as an intermediate (*51*). If a Tyr residue is placed in the proximity of the Fe(III)−O_2^- heme, reduction of superoxide to water easily takes place with a proton of tyrosine, and the resultant tyrosinate would be bound to an Fe(III) ion. The tyrosinate would pull the Fe ion together with heme toward the F helix and would cleave the Fe−E7-His bond.

Recently sequences of 700 globins, including 146 non-vertebrate hemoglobins, were aligned on the basis of the conservation of secondary structures and the avoidance of gap penalties (*52*). In all hemoglobins, F8-His was absolutely conserved. The E7-His was also conserved in vertebrate hemoglobins, but it was replaced by Gln, Val, or Tyr in some of nonvertebrate hemoglobins (*53*). It is possible that E7-Tyr in platyhelminths hemoglobins binds to a heme as the sixth ligand in the same oxidation process as for Hb M Iwate.

Low Oxygen Affinity of Hb M Iwate. Three likely communication pathways of a structural change from the α to β hemes have been proposed by Ho (*54*). In all of them, a change of the Fe−His bond of α heme is a trigger for the quaternary structure transition. Recent NMR (*54*), EPR (*55*), and UV resonance Raman (*56*) studies have demonstrated that the Fe−His bond in the α subunit is indispensable for the occurrence of the R → T transition of hemoglobin. In nitrosyl hemoglobin (NOHb), addition of IHP at low pH causes the cleavage of the Fe−His(F8) bond in the α subunit (*55*), and then the Hb conformation is biased for the T structure. The α(porphyrin),β(Fe heme)Hb adopts the T structure at low pH regardless of ligation in the β subunit, because of the absence of the Fe−His bond in the α heme (*57*). Thus, the lack of the Fe−His(F8) bond in the abnormal α subunit is probably a main reason for keeping the quaternary structure of Hb M Iwate in the T structure.

REFERENCES

1. Shibata, S., Miyaji, T., Iuchi, I., and Tamura, A. (1967) *Acta Haematol. Jpn. 27*, 13−18.
2. Greer, J. (1971) *J. Mol. Biol. 59*, 107−126.
3. Peisach, J., and Gersonde, K. (1977) *Biochemistry 16*, 2539−2545.
4. La Mar, G. N., Nagai, K., Jue, T., Budd, D. L., Gersonde, K., Sick, H., Kagimoto, T., Hayashi, A., and Taketa, F. (1980) *Biochem. Biophys. Res. Commun. 96*, 1172−1177.
5. Nagai, K., Kagimoto, T., Hayashi, A., Taketa, F., and Kitagawa, T. (1983) *Biochemistry 22*, 1305−1311.
6. Nagai, M., Yoneyama, Y., and Kitagawa, T. (1989) *Biochemistry 28*, 2418−2422.
7. Nagai, M., Yoneyama, Y., and Kitagawa, T. (1991) *Biochemistry 30*, 6495−6503.
8. Aki, M., Ogura, T, Shinzawa-Itoh, K., Yoshikawa, S., and Kitagawa, T. (2000) *J. Phys. Chem.*, in press.
9. Nagai, M., Kaminaka, S., Ohba, Y., Nagai, Y., Mizutani, Y., and Kitagawa, T. (1995) *J. Biol. Chem. 270*, 1636−1642.
10. Nagai, M., Yubisui, T., and Yoneyama, Y. (1980) *J. Biol. Chem. 255*, 4599−4602.
11. Bucci, E., and Fronticelli, C. (1965) *J. Biol. Chem. 240*, PC551−552.
12. Bucci, E. (1981) *Methods Enzymol. 76*, 97−106.
13. Banerjee, R., Stetzkowski, F., and Henry, Y. (1973) *J. Mol. Biol. 73*, 455−467.
14. Hendra, P. J., and Loader, E. J. (1908) *Chem. Ind. (London)* 718−719.
15. Harada, I., Miura, T., and Takeuchi, H. (1986) *Spectrochim. Acta 42A*, 307−312.
16. Miura, T., Takeuchi, T., and Harada, I. (1988) *Biochemistry 27*, 88−94.
17. Miura, T., Takeuchi, T., and Harada, I. (1989) *J. Raman Spectrosc. 20*, 667−671.
18. Rodgers, K. R., Su, C., Subramanian, S., and Spiro, T. G. (1992) *J. Am. Chem. Soc. 114*, 3679−3709.
19. Hu, X., and Spiro, T. G. (1997) *Biochemistry 36*, 15701−15712.
20. Nagai, M., Wajcman, H., Lahary, A., Nakatsukasa, T., Nagatomo, S., and Kitagawa, T. (1999) *Biochemistry 38*, 1243−1251.
21. Kitagawa, T., and Ozaki, Y. (1987) *Struct. Bonding 64*, 71−115.
22. Spiro, T. G. (1983) in *Iron Porphyrins* (Lever, A. B. P., and Gray, H., Eds.) Vol. 2, pp 89−159, Addison-Wesley, Reading, MA.
23. Felton, R. H., Roman, A. Y., and Yu, N.-T. (1976) *Biochim. Biophys. Acta 434*, 82−89.
24. Spiro, T. G., and Burke, M. J. (1976) *J. Am. Chem. Soc. 98*, 5482−5489.
25. Kitagawa, T., Kyogoku, Y., Iizuka, T., and Saito, M. I. (1976) *J. Am. Chem. Soc. 98*, 5169−5173.
26. Spiro, T. G., Slong, I. D., and Stein, P. (1979) *J. Am. Chem. Soc. 101*, 2648−2655.
27. Teraoka, J., and Kitagawa, T. (1980) *J. Phys. Chem. 84*, 1928−1935.

28. Jayaraman, V., and Spiro, T. G. (1996) *Biospectroscopy 2*, 311−316.
29. Hu, S., Smith, K. M., and Spiro, T. G. (1996) *J. Am. Chem. Soc. 118*, 12638−12646.
30. Choi, S., and Spiro, T. G. (1983) *J. Am. Chem. Soc. 105*, 3683−3692.
31. Argade, P., Sassaroli, M., Rousseau, D. L., Inubushi, T., Ikeda-Saito, M., and Lapidat, A. (1984) *J. Am. Chem. Soc. 106*, 6593−6596.
32. Ozaki, Y., Kitagawa, T., and Kyogoku, Y. (1976) *FEBS Lett. 69*, 369−372.
33. Yamamoto, T., Palmer, G., Gill, D., Salmon, I. T., and Rimai L. (1973) *J. Biol. Chem. 248*, 5211−5213.
34. Matsukawa, S., Mawatari, K., Yoneyama, Y., and Kitagawa, T. (1985) *J. Am. Chem. Soc. 107*, 1108−1113.
35. Smulevich, G., Hu, S., Rodgers, K. R., Goodin, D. B., Smith, K. M., and Spiro, T. G. (1996) *Biospectroscopy 2*, 365−376.
36. Teraoka, J., and Kitagawa, T. (1981) *J. Biol. Chem. 256*, 3969−3977.
37. Hayashi, A., Shimizu, A., Yamamura, Y., and Watari, H. (1965) *Biochim. Biophys. Acta 102*, 626−628.
38. Tatsuno, Y., Saeki, Y., Iwaki, M., Yagi, T., Nozaki, M., Kitagawa, T., and Otsuka, S. (1978) *J. Am. Chem. Soc. 100*, 4614−4615.
39. Austin, J. C., Rodgers, K. R., and Spiro, T. G. (1993) *Methods Enzymol. 226*, 374−396.
40. Nagai, M., Imai, K., Kaminaka, S., Mizutani, Y., and Kitagawa, T. (1996) *J. Mol. Struct. 379*, 65−75.
41. Hildebrandt, P. G., Copland, R. A., and Spiro, T. G. (1988) *Biochemistry 27*, 5426−5433.
42. Adachi, S., Nagano, S., Ishimori, K., Watanabe, Y., and Morishima, I. (1993) *Biochemistry 32*, 241−252.
43. Egeberg, K. D., Springer, B. A., Martinis, S. A., and Sliger, S. G. (1990) *Biochemistry 29*, 9783−9791.
44. Hildebrand, D. P., Burk, D. L., Maurus, R., Ferrei, J. C., Brayaer, G. D., and Mauk, A. G. (1995) *Biochemistry 34*, 1997−2005.
45. Nissum, M., Neri, F., Mandelman, D., Poulus, T. L., and Smulevich, G. (1998) *Biochemistry 37*, 8080−8087.
46. Peterson, E. S., Friedman, J. M., Chien, E. Y. T., and Sliger, S. G. (1998) *Biochemistry 37*, 12301−12319.
47. Walde, G. S., and Theil, E. C. (1993) *Biochemistry 32*, 13262−13269.
48. Walde, G. S., Ling, J., Sanders-Loehr, J., and Theil, E. C. (1993) *Science 259*, 796−798.
49. Nagai, M., Mawatari, K., Nagai, Y., Horita, S., Yoneyama, Y., and Hori, H. (1995) *Biochem. Biophys. Res. Commun. 210*, 483−490.
50. Dong, A., Nagai, M., Yoneyama, Y., and Caughey, W. S. (1994) *J. Biol. Chem. 269*, 25365−25368.
51. Momenteau, M., and Reed, C. A. (1994) *Chem. Rev. 94*, 659−698.
52. Kapp, O. H., Moens, L., Vanfleteren, J., Trotman, C. N., Suzuki, T., and Vinogradov, S. N. (1995) *Protein Sci. 4*, 2179−2190.
53. Suzuki, T., and Imai, K. (1998) *Cell Mol. Life Sci. 54*, 979−1004.
54. Ho, C. (1992) *Adv. Protein Chem. 43*, 152−312.
55. Yonetani, T., Tsuneshige, A., Zhou, Y., and Chen, X. (1998) *J. Biol. Chem. 273*, 20323−20333.
56. Nagatomo, S., Nagai, M., Tsuneshige, A., Yonetani, T., and Kitagawa, T. (1999) *Biochemistry 38*, 9659−9666.
57. Fujii, M., Hori, H., Miyazaki, G., Morimoto, H., and Yonetani, T. (1993) *J. Biol. Chem. 268*, 15386−15393.

BI001029I